REPORT DOCUMENTATION PAGE

Form Approved OMB NO. 0704-0188

1. REPORT DATE (DD-MM-YYYY)	2. REPORT TYPE	3. DATES COVERED (From - To)
	New Reprint	-

4. TITLE AND SUBTITLE
Synthesis of large-pore stabilized MIL-53(Al) compounds with increased CO2 adsorption and decreased water adsorption

5a. CONTRACT NUMBER
W911NF-10-1-0076

5b. GRANT NUMBER

5c. PROGRAM ELEMENT NUMBER
622622

6. AUTHORS
W. Mounfield, K. S. Walton

5d. PROJECT NUMBER

5e. TASK NUMBER

5f. WORK UNIT NUMBER

7. PERFORMING ORGANIZATION NAMES AND ADDRESSES
Georgia Tech Research Corporation
505 Tenth Street NW

Atlanta, GA 30332 -0420

8. PERFORMING ORGANIZATION REPORT NUMBER

9. SPONSORING/MONITORING AGENCY NAME(S) AND ADDRESS (ES)
U.S. Army Research Office
P.O. Box 12211
Research Triangle Park, NC 27709-2211

10. SPONSOR/MONITOR'S ACRONYM(S)
ARO

11. SPONSOR/MONITOR'S REPORT NUMBER(S)
57994-CH.30

12. DISTRIBUTION AVAILIBILITY STATEMENT
Approved for public release; distribution is unlimited.

13. SUPPLEMENTARY NOTES
The views, opinions and/or findings contained in this report are those of the author(s) and should not contrued as an official Department of the Army position, policy or decision, unless so designated by other documentation.

14. ABSTRACT
Abstract included in file.

15. SUBJECT TERMS
breathing MOFs, solvent effects

16. SECURITY CLASSIFICATION OF:			17. LIMITATION OF ABSTRACT	15. NUMBER OF PAGES	19a. NAME OF RESPONSIBLE PERSON
a. REPORT	b. ABSTRACT	c. THIS PAGE			Krista Walton
UU	UU	UU	UU		19b. TELEPHONE NUMBER: 404-894-5254

Report Title

Synthesis of large-pore stabilized MIL-53(Al) compounds with increased CO2 adsorption and decreased water adsorption

ABSTRACT

Abstract included in file.

REPORT DOCUMENTATION PAGE (SF298)
(Continuation Sheet)

Continuation for Block 13

ARO Report Number 57994.30-CH
Synthesis of large-pore stabilized MIL-53(Al) co...

Block 13: Supplementary Note

Approved for public release; distribution is unlimited.

Journal of Materials Chemistry RSCPublishing

ARTICLE

Synthesis of Large-Pore Stabilized MIL-53(Al) Compounds with Increased CO_2 Adsorption and Decreased Water Adsorption

Cite this: DOI: 10.1039/x0xx00000x

William P. Mounfield, III[a] and Krista S. Walton[a]

Received 00th January 2012,
Accepted 00th January 2012

DOI: 10.1039/x0xx00000x

www.rsc.org/

This work reports two large-pore stabilized MIL-53(Al) metal-organic frameworks prepared via solvothermal synthesis strategies that possess no or only slight breathing behaviour. Powder X-ray diffraction confirmed one material remains in the large-pore form under all conditions, while the other material undergoes a more gradual breathing transition than is observed for MIL-53(Al) prepared by traditional methods. Solid-state NMR was employed to elucidate additional structural information and gain insight into the role synthesis solvent plays on breathing behaviour. The CO_2 and water adsorption of these large-pore stabilized materials were studied, and the improvement in CO_2 loadings over MIL-53(Al) prepared by traditional methods was discussed.

Introduction

Metal-organic frameworks (MOFs) are a promising class of materials that have garnered much research attention for their potential applications. These inorganic-organic hybrid materials are characterized by metal clusters and organic linkers, large surface areas, and tunable chemical properties that make them excellent candidates for gas separations.[1-8] Certain MOFs offer unique separation applications due to their ability to 'breathe', i.e., undergoing a breathing transition in the presence of certain guest molecules.[9-13] MIL-53 is one of the most well-known MOFs that exhibits this breathing transition during specific guest molecule adsorption and has been studied extensively since its discovery in 2002.[14-22] Traditionally synthesized in water, MIL-53(Al) is comprised of $AlO_4(OH)_2$ corner-sharing octahedral chains connected by terephthalate groups to form a three-dimensional structure with 8.5 Å pores.[15] Despite the wide research into its breathing behaviours, there has been much less attention given to understanding the effect of solvent on the synthesis and breathing behaviour of MIL-53(Al). DMF (*n,n*-dimethylformamide) is commonly used in MIL series MOF synthesis such as the amine-functionalized MIL-53(Al)[23], as well as its polymorph MIL-101(Al)-NH_2.[24] In addition, a study on the synthesis of the non-porous MIL-69[25] found that the use of DMF as solvent in place of water allowed the formation of a new porous material, DUT-4.[26] However, despite its wide use in this and many other MOF syntheses, to the authors' knowledge, there has not been a complete study on the effect of DMF on the synthesis and breathing behaviour of MIL-53(Al). Recently, a computational and experimental study of the amine-functionalized MIL-53(Al), MIL-101(Al) system investigated the effect of replacing water with DMF during synthesis and found DMF was essential for synthesis of the amine functionalized MIL-101(Al) material.[27] In this study, we present two solvothermal synthesis methods for MIL-53(Al) with DMF as the solvent. The synthesis at lower temperature results in a material that is stabilized in the large-pore (lp) form, similar to the non-breathing vanadium analogue, MIL-47(V),[16, 28] and exhibits higher CO_2 adsorption in the 1-20 bar pressure range and lower water adsorption at humidity levels less than 50 %RH in comparison to that of the breathing material synthesized by traditional routes. The synthesis at higher temperature results in a material that is stabilized in the lp form, but exhibits a swift breathing transition with higher CO_2 adsorption across the entire pressure range and much lower water adsorption at all humidity levels in comparison to that of the breathing material synthesized by traditional routes as well as the lower temperature, lp stabilized material presented in this study.

Experimental section

Synthesis of MIL-53(Al) materials

Synthesis of MIL-53(Al)$_{sDMF120}$. The synthesis of MIL-53(Al)$_{sDMF,120}$ (sDMF$_{120}$) was performed by mixing aluminium nitrate nonahydrate ($Al(NO_3)_3{\cdot}9H_2O$) and benzene-1,4-dicarboxylic acid (C_6H_4-1,4-$(CO_2H)_2$) (referred to as BDC hereafter) in a 1:2.25 molar ratio. The reagents were added to 30 mL DMF (n,n-dimethylformamide) and stirred for 30 minutes until all solids were dissolved. The mixture was placed in a 60 mL glass vial and reacted at isothermal conditions of

120°C for 72 hours. The resulting milky-white solid was gravity-filtered, washed with DMF three times and washed finally with methanol once. The final product was dried in air overnight.

Synthesis of MIL-53(Al)$_{sDMF120}$. The synthesis of MIL-53(Al)$_{sDMF,220}$ (sDMF$_{220}$) was performed by mixing aluminum nitrate nonahydrate ($Al(NO_3)_3{\cdot}9H_2O$) and benzene-1,4-dicarboxylic acid (C_6H_4-1,4-$(CO_2H)_2$) (referred to as BDC hereafter) in a 1:2.25 molar ratio. The reagents were added to 30 mL DMF (*n,n*-dimethylformamide) and stirred for 30 minutes until all solids were dissolved. The mixture was placed in a sealed Teflon-lined reactor and reacted at isothermal conditions of 220°C for 72 hours. The resulting white solid was gravity-filtered, washed with DMF three times and washed finally with methanol once. The final product was dried in air overnight.

Synthesis of MIL-53(Al)$_{sH2O}$. The synthesis of MIL-53(Al)$_{sH2O}$ (sH$_2$O) was performed following the procedure found in literature.[15] 1.30 g $Al(NO_3)_3$ and 0.288 g BDC were stirred for 30 minutes in 5 mL H_2O and placed in a 23 mL Teflon-lined stainless steel autoclave for 72 hours at 220°C. The resulting white product was gravity filtered and washed with water three times. Powder X-ray diffraction and nitrogen adsorption analysis were performed on the resulting white solid. Unreacted BDC was found in the pores, and an extraction process from literature was adapted to remove this leftover material.[17] The filtered product was placed in 10 mL DMF in a 23 mL Teflon-lined stainless steel autoclave overnight at 150°C. The resulting product was filtered with DMF and dried in air overnight.

Powder X-ray diffraction

Powder X-ray diffraction patterns were recorded on an X'Pert X-ray PANalytical diffractometer with an X'accelerator module using Cu Kα (λ = 1.5418 Å) radiation at room temperature, with a step size of 0.02˚ in two theta (2θ). All attempts at obtaining single crystal X-ray diffraction data were unsuccessful.

N_2 physisorption

Nitrogen physisorption isotherms were measured at 77 K for samples activated at 473K for 16h before and after water exposure using the Quadrasorb system from Quantachrome instruments (Fig. S2). Nitrogen adsorption analysis was performed on all resulting products, and surface areas were determined by applying BET theory over a range of data points applicable to microporous materials.[29] N_2 isotherms showed typical Type I behaviour as per the IUPAC classification.

Gas adsorption

An Intelligent Gravimetric Analyzer (IGA-1 series, Hiden Analytical Ltd.) was used to collect pure gas (CO_2, CH_4, N_2) adsorption isotherms at 293K and pressures up to 20 bar (Figure 3, S3). Samples were activated in situ at 473 K under vacuum until no further weight loss was observed. After activation, the system was maintained under vacuum, and the temperature was adjusted to the desired value. A sample size of approximately 25 mg was used for the measurements, and a maximum equilibration time of 40 min was used for each point in the isotherm.

Water adsorption

An Intelligent Gravimetric Analyzer (IGA-3 series, Hiden Analytical Ltd.) was used to obtain water vapour adsorption isotherms at 293K (Figure 4). A sample size of approximately 35 mg was used for collecting the water vapour adsorption isotherm. Dry air was used as the carrier gas, with a percentage being bubbled through a vessel filled with deionized water. Two mass flow controllers were used to vary the ratio of saturated air and dry air so that the relative humidity (%RH) could be controlled. Due to water condensation in the equipment at higher humidities, experiments were conducted up to 80 %RH. The total gas flow rate was set at 200 cm3/min, and each adsorption/desorption step was allowed a maximum time of 24 h to approach equilibrium. Samples were activated in situ at 473 K under vacuum until no further weight loss was observed before starting the experiment. Samples were regenerated by heating at 473 K under vacuum for 16 h after the water adsorption isotherm measurement prior to BET analysis.

FTIR spectroscopy

FTIR spectra were recorded on a Bruker Vertex 70, equipped with a DTGS detector in transmission geometry. Samples were prepared in a 1:100 sample:KBr pellet. The spectra were collected with an accumulation of 24 scans and a resolution of 4 cm^{-1}. A flow of N_2 at 20 mL min^{-1} was maintained during the measurement. The spectra were recorded at room temperature without any pre-treatment of the samples.

Solid-state NMR spectroscopy

^{27}Al, ^{13}C, and ^{1}H NMR spectra were recorded on a Bruker Avance III spectrometer with a 9.4T magnetic field operating at 400 MHz using an automated procedure for analysis. A 4mm Bruker MAS probe with a ZrO_2 rotor spinning at 12 kHz was used in the ^{1}H and ^{27}Al MAS NMR studies. ^{27}Al MAS NMR spectra were recorded over 4096 scans on a simple block decay single-pulse excitation of 0.6 μs pulse duration with a repetition delay of 500 ms. Deconvolution of the ^{27}Al NMR spectra was performed using Bruker TopSpin 3.2.

Results and discussion

Due to the larger kinetic diameter in comparison to water, 5.5 Å versus 2.6 Å,[30] and its known ability to induce a large-pore structural transition,[31] DMF offers the ability to stabilize the lp form of MIL-53(Al) much like CO_2, which possesses a kinetic diameter of 3.6 Å. Recently, there has been work on alternative synthesis using an ionic liquid as the solvent in place of water for increasing the hydrophobicity of MIL-53.[32] The ionic liquid possesses a kinetic diameter similar to DMF, illustrated in Fig. S5. Therefore, in accordance with the findings of Liu et al.[32] and Senkovska et al.,[26] we hypothesized that the size of the

solvent molecule directs the synthesis such that DMF prevents the formation of the original literature framework, as illustrated in Fig. 1(c), where DMF molecules in orthogonal and parallel orientations are seen to block the pores and occupy a much larger space than the water molecule in Fig. 1(a). As seen by Senkovska et al. for DMF synthesis of MIL-69,[26] the framework must assemble in the lp form in the presence of DMF to accommodate the larger solvent molecule[14] as shown in Fig. 1(b), and when synthesized at lower temperatures (120 °C) is unable to undergo the breathing transition shown in Fig. 1(a) for dehydration/hydration/cooling of MIL-53(Al) materials prepared by published procedures.[15] Interestingly, synthesis at higher temperatures (220 °C) results in a material that is able to undergo a breathing transition similar to that observed for MIL-53(Al) in literature.[15]

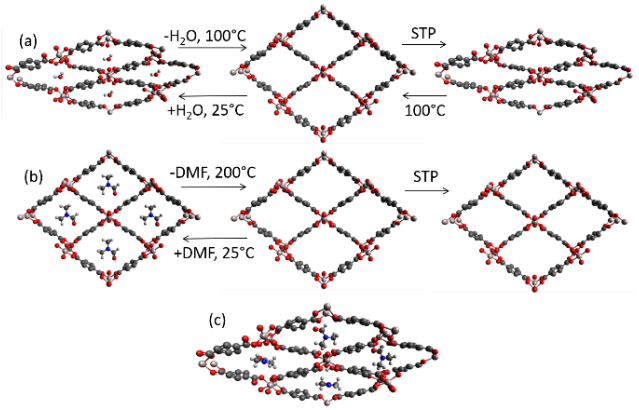

Fig. 1 Schematic of (a) MIL-53(Al)$_{sH2O}$ dehydration, hydration and cooling to room temperature after activation, (b) removal of DMF from pores of MIL-53(Al)$_{sDMF}$ and stability of lp form after cooling to room temperature (c) DMF molecules occupying pore space of MIL-53(Al)$_{sH2O}$ in orthogonal and parallel orientations.

BET analysis was performed on each of the resulting products and it was determined that the unreacted BDC was removed from the sH_2O material by the DMF extraction process and no calcination step was necessary. Further, the extraction step allows for one of the highest reported BET surface areas for MIL-53(Al), 1410 m^2/g, much higher than previously reported literature values.[15, 18, 33, 34] In comparison, $sDMF_{120,220}$ possess activated surface areas of 1472 m^2/g, and 1570 m^2/g, respectively. In order to determine the degree to which the three materials were activated, the theoretical surface area was calculated and compared to the experimental surface area results.[35] As all surface areas are nearing the theoretical value of 1632.8 m^2/g, it was believed that the materials were sufficiently activated. However, analysis of FTIR spectra (Fig. 2) for $sDMF_{220}$ showed the presence of a spectral peak at 1660 cm^{-1} attributed to ν(C=O) in DMF molecules that remain trapped in the material; an observation that has been made in other MOFs when using DMF in place of H_2O as the synthesis solvent.[36] Several washing steps with methanol were repeated in an attempt to remove the DMF molecules from the framework; however, it was found that these repeated washing steps did not remove the trapped species, suggesting these molecules are coordinated to the metal center or to the benzene ring of the ligand. Although there are some coordinated DMF molecules in the material, the observed high surface area indicates that these molecules are few in number and should not reduce the material's gas adsorption capability.

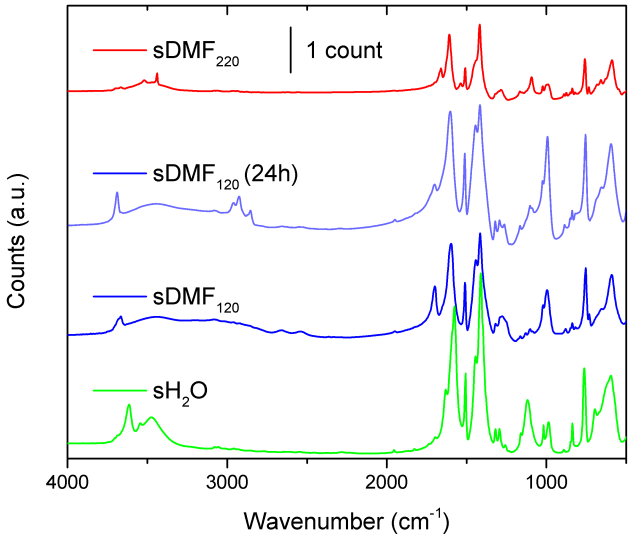

Fig. 2 FTIR spectra of activated MIL-53(Al)$_{sH2O}$ (sH_2O, green), activated MIL-53(Al)$_{sDMF,120}$ ($sDMF_{120}$, blue), MIL-53(Al)$_{sDMF,120}$ ($sDMF_{120}$ 24h, light blue) activated for 24 hours at 300 °C after six methanol washes, activated MIL-53(Al)$_{sDMF,220}$ ($sDMF_{220}$, red).

Analysis of FTIR spectra for $sDMF_{120}$ showed the presence of a spectral peak at 1701 cm^{-1} attributed to ν(COOH) in terephthalate linkers in the material. Several washing steps with methanol were repeated in an attempt to remove any free, unreacted BDC molecules from the framework, but these repeated washing steps did not eliminate the presence of the spectral peak in the FTIR spectra. In order to confirm the peak was not due to free BDC molecules trapped in $sDMF_{120}$, the material was again washed six times with methanol and activated at 300°C for 24 hours. A BET analysis confirmed a complete structural collapse of the material and the continued presence of the spectral peak at 1706 cm^{-1} indicates a free carboxylic group of BDC still exists within the material and cannot be removed through activation. Furthermore, the continued presence of this group after numerous activation procedures, suggests that this peak is not, in fact, due to trapped BDC molecules, but rather an indication of the defects of the material, i.e., uncoordinated linkers that contribute to the framework's inability to undergo a structural transition.

Irretrievably trapped terephthalate molecules are not observed for the $sDMF_{220}$ material; the absence of a peak near 1700 cm^{-1} in Fig. 2, confirms complete removal of BDC molecules.[37-40] As DMF molecules cannot be completely removed from $sDMF_{220}$ through the activation procedure described, and the framework undergoes a complete but gradual breathing transition, the framework appears to assemble differently than the literature framework due to the larger

solvent molecule. This hypothesis is supported by the slightly larger cell parameters observed with LeBail refinement (Figure S8, Table S1). Adsorbed water molecules in sH_2O material account for the spectral band observed at 1629 cm^{-1}.

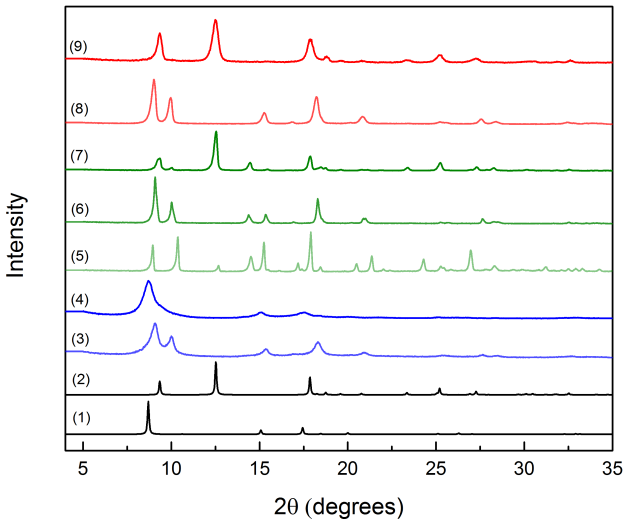

Fig. 3 XRD patterns of (1) large-pore form, (2) narrow-pore form, (3) as-synthesized MIL-53(Al)$_{sDMF,120}$, (4) activated MIL-53(Al)$_{sDMF,120}$, (5) as-synthesized MIL-53(Al)$_{sH2O}$, (6) extracted MIL-53(Al)$_{sH2O}$, (7) activated MIL-53(Al)$_{sH2O}$ (8) as-synthesized MIL-53(Al)$_{sDMF,220}$, (9) activated MIL-53(Al)$_{sDMF,220}$.

Powder X-ray diffraction (XRD) was used to verify the structures of the three MIL-53(Al) micro-crystalline powders. Fig. 3 shows that the sample synthesized with DMF at low temperatures, designated as MIL-53(Al)$_{sDMF,120}$, exhibits broad, well-resolved peaks, indicating small crystallites, as seen in the recent work with ionothermal synthesis.[32] After activation, it is evident that MIL-53(Al)$_{sDMF,120}$ is present in only the large-pore (lp) form.[15] The stability of MIL-53(Al)$_{sDMF,120}$ in the lp form is quite unlike the MIL-53(Al) sample synthesized with water, designated MIL-53(Al)$_{sH2O}$, as seen when referencing its as-synthesized XRD pattern, Fig. 3(5). After extraction of remaining BDC molecules from the pores of the sample, and subsequent activation, it is clear that the MIL-53(Al)$_{sH2O}$ sample is present in the narrow-pore (np) form.[15] The material synthesized at higher temperatures in DMF, designated as MIL-53(Al)$_{sDMF,220}$, exhibits an as-synthesized pattern similar to MIL-53(Al)$_{sH2O}$ after extraction with DMF, where both materials are present in the lp form. However, after activation, unlike the material synthesized in DMF at lower temperatures, MIL-53(Al)$_{sDMF,220}$ is present in the np form, similar to MIL-53(Al)$_{sH2O}$. In conjunction with the presence of DMF in the IR spectra from the activated MIL-53(Al)$_{sDMF,220}$ sample, we hypothesized that the material would be able to undergo a complete structural transition similar to the literature framework but that the transition would be affected by the coordinated DMF molecules; a hypothesis that is tested with gas adsorption experiments later in the text. The LeBail refinement performed on the PXRD pattern for MIL-53(Al)$_{sDMF,220}$ reveals the material exists in a structural form that is slightly larger than the traditional material's np form. After intermittent exposure to laboratory atmosphere, ~50 %RH, there was no observed change in the samples' XRD pattern, as seen in Fig. S4.

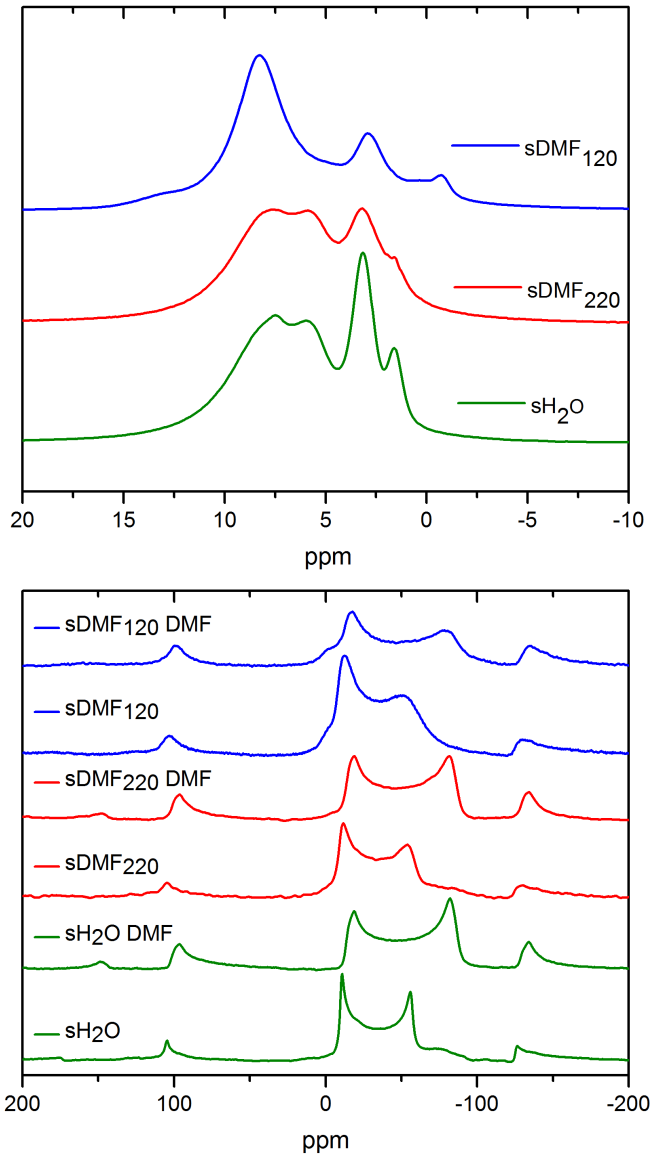

Fig. 4 (top) ^{1}H, and (bottom) ^{27}Al MAS NMR spectra for $sDMF_{120}$ (blue), $sDMF_{220}$ (red), and sH_2O (green).

A combination of ^{27}Al, ^{13}C, and ^{1}H MAS NMR was used to elucidate further structural information for the three MIL-53(Al) micro-crystalline powders. The ^{13}C MAS NMR spectra of sH_2O and $sDMF_{220}$ in Fig. S6 exhibit three lines at δ = 130, 137, and 175 ppm, where the signal at δ = 174 ppm can be identified as the carboxylic group interacting with a water molecule. The ^{13}C MAS NMR spectra are quite similar for these materials and no clear difference with regards to structural properties under hydrated conditions can be discerned. However, ^{1}H MAS NMR has been used previously to evaluate the hydration of MIL-53(Al) compounds,[15, 41] and it allows the

determination of the relative hydrophobicity of the materials. The signal at δ = 3 ppm in the ^{1}H MAS NMR spectra in Fig. 4 for $sDMF_{120}$, $sDMF_{220}$, and sH_2O is indicative of the formation of weak hydrogen bonds between water molecules and neighbouring oxygen atoms of the organic linkers. The increased intensity of this signal in sH_2O clearly illustrates the traditionally synthesized sample is hydrated to a greater degree when exposed to laboratory air than the samples synthesized in DMF at high temperature. In addition, the absence of the water signal at 6.1 ppm in the $sDMF_{120}$ spectrum indicates a very low degree of hydration due to the materials permanent state in the large pore form.

To further analyse the MIL-53(Al) materials' structural properties, ^{27}Al MAS NMR was performed on activated samples and compared to samples in the presence of DMF. The ^{27}Al spectra for activated $sDMF_{120}$ exhibits a quadrupolar pattern with δ_{27Al} = 3.3 ppm, C_Q = 8.2 MHz, η_Q = 0.2, $sDMF_{220}$ features a well-defined quadrupolar pattern with δ_{27Al} = 3.6 ppm, C_Q = 8.4 MHz, η_Q = 0.13, while the spectrum for sH_2O exhibits a quadrupolar pattern with δ_{27Al} = 2.9 ppm, C_Q = 8.1 MHz, η_Q = 0.08 and no trace of any other aluminium-containing phase, confirming there is no remaining amorphous $Al(OH)_3$. In order to analyse the breathing transition of $sDMF_{220}$ and sH_2O, the activated materials were saturated with DMF to place them in their lp form. The ^{27}Al MAS spectrum for $sDMF_{120}$ features a single quadrupolar pattern with δ_{27Al} = 11 ppm, C_Q = 10.1 MHz, η_Q = 0.16, $sDMF_{220}$ features a quadrupolar pattern with δ_{27Al} = 5 ppm, C_Q = 10.1 MHz, η_Q = 0.098, while the spectrum for sH_2O exhibits a quadrupolar pattern with δ_{27Al} = 3.6 ppm, C_Q = 10.1 MHz, η_Q = 0.1. The smaller increase in the quadrupolar coupling constant upon saturation with DMF for $sDMF_{220}$, 8.4~10.1, and $sDMF_{120}$, 8.2~10.1 compared to the increase in C_Q for sH_2O, 8.1~10.1, can be attributed to a decrease in the strain on the $AlO_4(OH)_2$ octahedra in the materials synthesized in DMF. As the octahedra experience less strain in the materials synthesized in DMF, they are able to gradually transition from closed to open pore forms in the case of $sDMF_{220}$, or remain in the open pore form permanently in the case of $sDMF_{120}$ as is confirmed with CO_2 adsorption experiments.

After analysing the PXRD and solid-state NMR results and concluding the MIL-53(Al)$_{sDMF,120,220}$ samples are unique MIL-53(Al) materials, further investigation of their structure and behaviour was made with high pressure, pure-component CO_2 and CH_4 adsorption experiments. The CO_2 and CH_4 adsorption isotherms for $sDMF_{120}$ shown in Fig. 5 exhibit Type I isotherms with no hysteresis. CO_2 is more strongly adsorbed than CH_4 as it has a higher quadrupole moment than the nonpolar methane. The CH_4 adsorption isotherms for sH_2O and $sDMF_{220}$ shown in Fig. 5 also exhibit Type I behaviour. The CO_2 adsorption isotherm for sH_2O exhibits strong Type IV behaviour with large hysteresis upon desorption, which is characteristic of the traditional breathing behaviour seen in literature.[16] The CO_2 isotherm for $sDMF_{220}$ exhibits a weak Type IV behaviour with small hysteresis upon desorption characteristic of a gradual structural transition, lacking the quick step-like change observed for CO_2 adsorption in sH_2O, resulting in the observation of only a slight breathing behaviour. The observation of this gradual breathing behaviour during CO_2 adsorption combined with the results from ^{27}Al NMR showing reduced strain on the octahedral metal centers while in the lp form supports the hypothesis presented previously that the $sDMF_{220}$ material is indeed able to undergo a complete structural transition, but with a more gradual movement between open and closed forms. In addition, the presence of the material in the np form after activation suggests the number of coordinated DMF molecules is not enough to induce a transition to the lp form without guest adsorption.

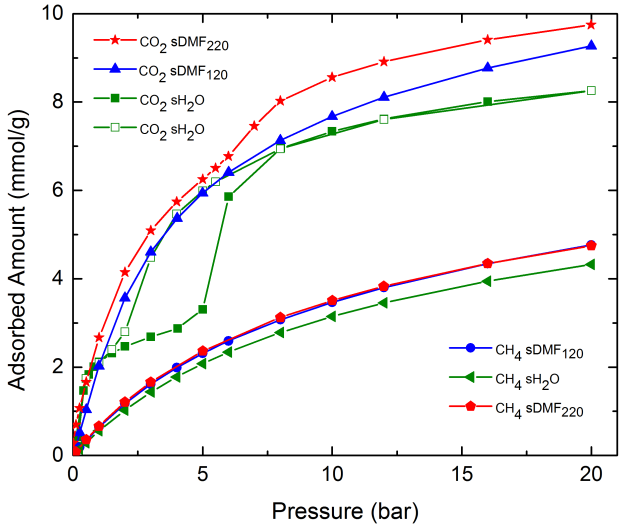

Fig. 5 CO_2 and CH_4 adsorption isotherms at 25°C for $sDMF_{220}$ (red stars and pentagons), $sDMF_{120}$ (blue triangles and circles) and sH_2O (green squares and left triangles) as a function of pressure ranging from 0-20 bar. Desorption isotherms are omitted except for sH_2O (open green squares), which shows large hysteresis.

The CO_2 and CH_4 adsorption observed for sH_2O, 8.2 mmol/g and 4.3 mmol/g, match that found in the literature, while the overall CO_2 loading for $sDMF_{120}$ is more than 1 mmol/g higher than sH_2O, 9.3 mmol/g. The CH_4 loading is only slightly increased by 0.5 mmol/g to 4.8 mmol/g. The CO_2 loading for $sDMF_{220}$ is more than 1.5 mmol/g higher than sH_2O, 9.8 mmol/g, while the CH_4 loading is the same as $sDMF_{120}$, 4.8 mmol/g. However, a much greater increase over sH_2O is observed for both materials synthesized in DMF in the 1-5 bar region. It is in this region that sH_2O is still present in the np form, and is unable to have additional significant adsorption, while $sDMF_{120}$ is stabilized in the lp form and has continued adsorption throughout this region. It is evident from the adsorption data that the $sDMF_{120}$ material is indeed present in the lp form throughout adsorption of CO_2 as it closely follows the desorption curve for sH_2O in the 2-5 bar region, where the sH_2O material is still present in the lp form before relaxing to the np form as the pressure drops below 2 bar. Contrary to the observations for the material synthesized at low temperatures in DMF in this intermediate pressure region, $sDMF_{220}$ undergoes a gradual structural transition to the lp form, as seen in Fig. 5 rather than the step breathing transition

observed in the sH_2O material, allowing for greatly increased adsorption throughout the region. The coordinated DMF molecules allow retention of the breathing ability of the framework and greatly increased CO_2 adsorption capacity in the transition region. Due to the large increase in CO_2 adsorption with a negligible increase in CH_4 adsorption in this region, the $sDMF_{220}$ and $sDMF_{120}$ materials offer a three-fold increase in working capacity for processes run in the 1-5 bar region, 3.6 mmol/g vs 1.2 mmol/g, in addition to increased CO_2 adsorption at 1 bar for $sDMF_{220}$, 2.7 mmol/g vs 2.1 mmol/g.

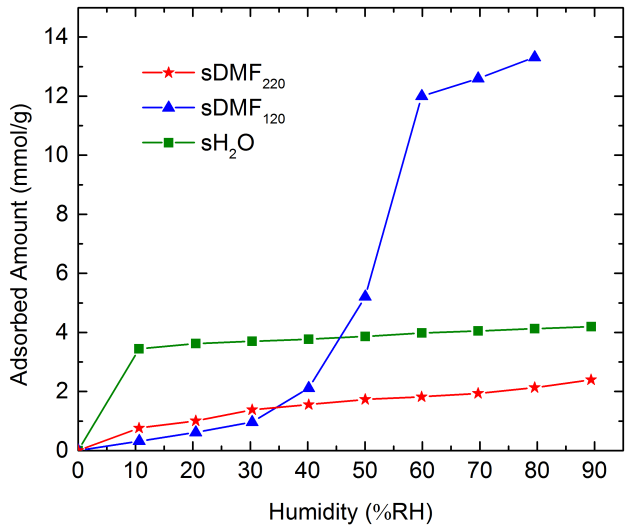

Fig. 6 H_2O adsorption isotherms at 25°C and 1 bar for $sDMF_{120}$ (blue circles), $sDMF_{220}$ (red squares) and sH_2O (green stars) as a function of relative humidity.

Due to the discovery of the non-breathing behaviour of $sDMF_{120}$, and the gradual breathing behaviour of $sDMF_{220}$ a further investigation of the materials' performance in the presence of water was performed in comparison to that of sH_2O. Water adsorption isotherms were obtained at 1 bar with relative humidity ranging from 0-90%. The water adsorption isotherm for the MIL-53(Al) material synthesized by traditional water synthesis shown in Fig. 6 (sH_2O) exhibits Type I behaviour typical of a small pore material with very little increase in loading after the initial adsorption of 4 mmol/g at 10 %RH. The material synthesized at low temperatures in DMF, $sDMF_{120}$, however, exhibits a Type V isotherm characteristic of a large-pore material, with very low initial loading until >50 %RH. $sDMF_{120}$ adsorbs less than 1 mmol/g of water vapour until the humidity rises above 30 %RH, and maintains a lower loading than sH_2O until 50 %RH. This low adsorption along with the absence of any change in PXRD pattern (Fig. S4) or BET surface area after routine exposure to laboratory atmosphere of similar humidity leads us to believe that the material is stable in humid conditions less than 50 %RH. The material synthesized at high temperatures in DMF, $sDMF_{220}$, however, exhibits an approximately linear isotherm, with very low loading across the entire range of humidity. $sDMF_{220}$ adsorbs less than 2 mmol/g of water vapour at 90 %RH, less than half the loading of sH_2O at the same humidity level. Coincident with the observation of DMF molecules remaining after activation in the FTIR spectra and the gradual breathing behaviour of $sDMF_{220}$ during CO_2 adsorption it is likely that the few coordinated DMF molecules prevent or reduce water adsorption around their locations in the framework resulting in low water adsorption and increased hydrophobicity, as well as continued low adsorption in the high humidity range similar to sH_2O with the np form preventing the clustering and adsorption of large amounts of water seen in $sDMF_{120}$. Similar exposure to laboratory air did not yield any change in the PXRD pattern or BET surface area of $sDMF_{220}$ as was expected from the ^1H NMR results demonstrating its greater hydrophobicity in room conditions than sH_2O.

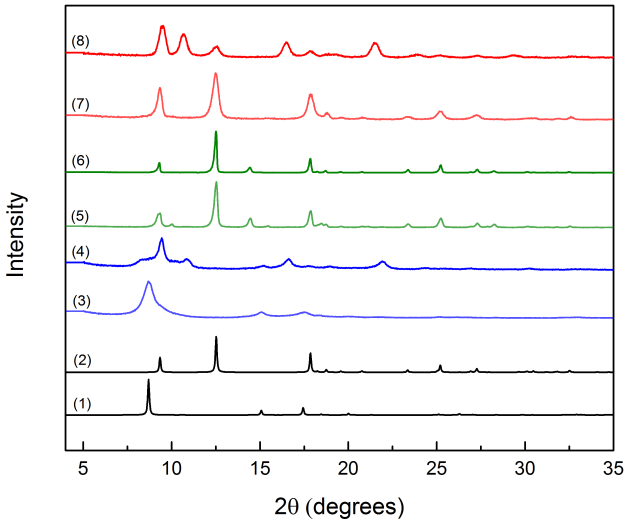

Fig. 7 XRD patterns of (1) large-pore form, (2) narrow-pore form, (3) activated $MIL\text{-}53(Al)_{sDMF,120}$, (4) post water adsorption $MIL\text{-}53(Al)_{sDMF,120}$, (5) activated $MIL\text{-}53(Al)_{sH2O}$, (6) post water adsorption $MIL\text{-}53(Al)_{sH2O}$, (7) activated $MIL\text{-}53(Al)_{sDMF,220}$, (8) post water adsorption $MIL\text{-}53(Al)_{sDMF,220}$.

In addition, we are able to gain insight into the water stability of the lp and np conformations of MIL-53(Al). It is evident that the continued water stability at higher relative humidity levels of the traditionally synthesized material stems from the immediate and complete pore filling with low water adsorption at initial humidity levels due to the presence of inaccessible areas of the pore volume while in the np form. Conversely, while $sDMF_{120}$ is in the lp form, water experiences weaker interactions with the pore surface at low humidity levels, as illustrated by the low initial adsorption until 50 %RH. However, as seen in experimental and computational studies of the effects of water on other MOFs,[42-44] beyond this point water clusters form and fill the pore, interacting more with the metal-ligand bond and leading to a breakdown of the structure as the material begins to adsorb large amounts of water, with an ultimate loading of 13.3 mmol/g. In addition, the presence of defects, indicated by FTIR analysis of this material, allows easy access to the metal-ligand bond and subsequent collapse of the structure. The large increase in adsorption in $sDMF_{120}$ corresponding to a breakdown of the MOF structure is

confirmed through comparison of PXRD patterns before and after water adsorption experiments shown in Fig. 7, and BET surface areas before and after water adsorption experiments. It is evident that a large change has occurred in the structure of $sDMF_{120}$ as the structure no longer resembles the activated pattern or the simulated lp or np form patterns and the BET surface area was reduced from 1472 m^2/g to 370 m^2/g.

$sDMF_{220}$, while appearing to behave similarly to sH_2O, is found to not be water stable, with the pattern after water adsorption experiments closely resembling its as-synthesized pattern shown in Fig. 3 (8), suggesting there are free BDC and $Al(OH)_x$ molecules present after being removed by attacking water molecules. The reduction of the BET surface area from 1570 m^2/g to 402 m^2/g confirms the breakdown of the framework in the presence of high humidity. The instability of this material, although present in a narrow-pore form, suggests that the coordinated DMF molecules may induce the observed larger np form which allows for enough water to be adsorbed to degrade the material. On the other hand, there is little change in the PXRD pattern for $MIL\text{-}53(Al)_{sH2O}$ after water adsorption, with the pattern closely resembling the activated pattern as well as the simulated np form. In addition, BET analysis showed a negligible change in surface area before and after water adsorption for $MIL\text{-}53(Al)_{sH2O}$, 1410 m^2/g to 1408 m^2/g, confirming the water stability of the material while in the np form. These results lead to the hypothesis that traditionally synthesized MIL-53(Al) materials as well as the large-pore stabilized materials are susceptible to water effects at high humidity levels while in pore forms any larger than the traditional np form, which would have a negative impact on CO_2 adsorption applications at higher pressures, where all types of these materials would be present in the large-pore form.

Conclusions

In conclusion, we have reported solvothermal syntheses of large-pore stabilized MIL-53(Al) MOFs that do not possess the standard breathing behaviour found in literature. Synthesis at lower temperature produces a material with no breathing behaviour, while synthesis at higher temperature results in a material with a gradual, slight breathing behaviour. The different breathing behaviour or lack thereof and increased stability of the large-pore form allows for a large increase in CO_2 adsorption in the 1-5 bar region, and overall loading for the large-pore only material, and a large increase throughout the entire pressure range for the gradually breathing MOF. Water adsorption studies of the $sDMF_{120}$ and $sDMF_{220}$ materials suggest that at humidity levels less than 50 %RH, the materials are stable and have much lower water loading than the sH_2O framework. It is evident that understanding and modulating the breathing behaviour of metal-organic frameworks offers unique opportunities for enhancing applications in gas adsorption, chemical sensing, and other areas of interest.

Acknowledgements

The authors thank Dr. Himanshu Jasuja, Nicholas Burtch, Dr. Michael A. Filler, and Saujan Sivaram for their valuable discussions. This material is based upon work supported by Army Research Office PECASE Award W911NF-10-0079 and ARO Contract W911NF-10-0076.

Notes and references

[a] School of Chemical and Biomolecular Engineering, Georgia Institute of Technology, 311 Ferst Drive NW, Atlanta, Georgia 30332, United States walton.chbe.gatech.edu; Email: krista.walton@chbe.gatech.edu

† The authors declare no competing financial interests. Electronic Supplementary Information (ESI) available: Experimental procedures, gas adsorption isotherms, XRD patterns, LeBail refinements, NMR spectra and TGA curves are included in the supporting information. See DOI: 10.1039/b000000x/

1. A. U. Czaja, N. Trukhan and U. Muller, *Chem. Soc. Rev.*, 2009, **38**, 1284-1293.
2. J. R. Li, R. J. Kuppler and H. C. Zhou, *Chem. Soc. Rev.*, 2009, **38**, 1477-1504.
3. S. Keskin, T. M. van Heest and D. S. Sholl, *ChemSusChem*, 2010, **3**, 879-891.
4. P. L. Llewellyn, S. Bourrelly, C. Vagner, N. Heymans, H. Leclerc, A. Ghoufi, P. Bazin, A. Vimont, M. Daturi, T. Devic, C. Serre, G. De Weireld and G. Maurin, *J. Phys. Chem. C*, 2013, **117**, 962-970.
5. G. D. Pirngruber, L. Hamon, S. Bourrelly, P. L. Llewellyn, E. Lenoir, V. Guillerm, C. Serre and T. Devic, *ChemSusChem*, 2012, **5**, 762-776.
6. B. Yilmaz, N. Trukhan and U. MÜLler, *Chin. J. Catal.*, 2012, **33**, 3-10.
7. R. E. Morris and P. S. Wheatley, *Angew. Chem.*, 2008, **47**, 4966-4981.
8. K. Sumida, D. L. Rogow, J. A. Mason, T. M. McDonald, E. D. Bloch, Z. R. Herm, T. H. Bae and J. R. Long, *Chem. Rev.*, 2012, **112**, 724-781.
9. L. Sarkisov, R. L. Martin, M. Haranczyk and B. Smit, *J. Am. Chem. Soc.*, 2014, **136**, 2228-2231.
10. P. L. Llewellyn, S. Bourrelly, C. Serre, Y. Filinchuk and G. Ferey, *Angew. Chem.*, 2006, **45**, 7751-7754.
11. G. Ferey and C. Serre, *Chem. Soc. Rev.*, 2009, **38**, 1380-1399.
12. B. Mu, F. Li, Y. G. Huang and K. S. Walton, *J. Mater. Chem.*, 2012, **22**, 10172-10178.
13. C. Serre, F. Millange, S. Surble and G. Ferey, *Angew. Chem.*, 2004, **43**, 6285-6289.
14. C. Serre, F. Millange, C. Thouvenot, M. Nogues, G. Marsolier, D. Louer and G. Ferey, *J. Am. Chem. Soc.*, 2002, **124**, 13519-13526.
15. T. Loiseau, C. Serre, C. Huguenard, G. Fink, F. Taulelle, M. Henry, T. Bataille and G. Ferey, *Chem-Eur J*, 2004, **10**, 1373-1382.
16. S. Bourrelly, P. L. Llewellyn, C. Serre, F. Millange, T. Loiseau and G. Ferey, *J. Am. Chem. Soc.*, 2005, **127**, 13519-13521.
17. C. Serre, S. Bourrelly, A. Vimont, N. A. Ramsahye, G. Maurin, P. L. Llewellyn, M. Daturi, Y. Filinchuk, O. Leynaud, P. Barnes and G. Férey, *Adv. Mater.*, 2007, **19**, 2246-2251.
18. P. Rallapalli, K. P. Prasanth, D. Patil, R. S. Somani, R. V. Jasra and H. C. Bajaj, *J. Porous Mater.*, 2010, **18**, 205-210.
19. R. I. Walton, A. S. Munn, N. Guillou and F. Millange, *Chem-Eur J*, 2011, **17**, 7069-7079.
20. F.-X. Coudert, A. Boutin, A. H. Fuchs and A. V. Neimark, *J. Phys. Chem. Lett.*, 2013, **4**, 3198-3205.
21. Y. Liu, J. H. Her, A. Dailly, A. J. Ramirez-Cuesta, D. A. Neumann and C. M. Brown, *J. Am. Chem. Soc.*, 2008, **130**, 11813-11818.

22. T. K. Trung, P. Trens, N. Tanchoux, S. Bourrelly, P. L. Llewellyn, S. Loera-Serna, C. Serre, T. Loiseau, F. Fajula and G. Ferey, *J. Am. Chem. Soc.*, 2008, **130**, 16926-16932.
23. S. Couck, J. F. Denayer, G. V. Baron, T. Remy, J. Gascon and F. Kapteijn, *J. Am. Chem. Soc.*, 2009, **131**, 6326-6327.
24. P. Serra-Crespo, E. V. Ramos-Fernandez, J. Gascon and F. Kapteijn, *Chem. Mater.*, 2011, **23**, 2565-2572.
25. T. Loiseau, C. Mellot-Draznieks, H. Muguerra, G. Férey, M. Haouas and F. Taulelle, *C. R. Chim.*, 2005, **8**, 765-772.
26. I. Senkovska, F. Hoffmann, M. Fröba, J. Getzschmann, W. Böhlmann and S. Kaskel, *Microporous Mesoporous Mater.*, 2009, **122**, 93-98.
27. M. G. Goesten, P. C. Magusin, E. A. Pidko, B. Mezari, E. J. Hensen, F. Kapteijn and J. Gascon, *Inorg. Chem.*, 2014, **53**, 882-887.
28. K. Barthelet, J. Marrot, D. Riou and G. Férey, *Angew. Chem.*, 2002, **41**, 281.
29. K. S. Walton and R. Q. Snurr, *J. Am. Chem. Soc.*, 2007, **129**, 8552-8556.
30. J. E. ten Elshof, C. R. Abadal, J. Sekulić, S. R. Chowdhury and D. H. A. Blank, *Microporous Mesoporous Mater.*, 2003, **65**, 197-208.
31. S. Biswas, T. Ahnfeldt and N. Stock, *Inorg. Chem.*, 2011, **50**, 9518-9526.
32. J. Liu, F. Zhang, X. Zou, G. Yu, N. Zhao, S. Fan and G. Zhu, *Chem. Commun.*, 2013, **49**, 7430-7432.
33. P. Rallapalli, D. Patil, K. P. Prasanth, R. S. Somani, R. V. Jasra and H. C. Bajaj, *J. Porous Mater.*, 2009, **17**, 523-528.
34. D. V. Patil, P. B. S. Rallapalli, G. P. Dangi, R. J. Tayade, R. S. Somani and H. C. Bajaj, *Ind. Eng. Chem. Res.*, 2011, **50**, 10516-10524.
35. T. Duren, F. Millange, G. Ferey, K. S. Walton and R. Q. Snurr, *J. Phys. Chem. C*, 2007, **111**, 15350-15356.
36. E. Tynan, P. Jensen, P. E. Kruger and A. C. Lees, *Chem. Commun.*, 2004, 776-777.
37. H. R. Moon, N. Kobayashi and M. P. Suh, *Inorg. Chem.*, 2006, **45**, 8672-8676.
38. M. Park, D. Moon, J. W. Yoon, J. S. Chang and M. S. Lah, *Chem. Commun.*, 2009, 2026-2028.
39. B. Mu, Y. G. Huang and K. S. Walton, *CrystEngComm*, 2010, **12**, 2347-2349.
40. H. Jasuja and K. S. Walton, *J. Phys. Chem. C*, 2013, **117**, 7062-7068.
41. Y. J. Jiang, J. Huang, S. Marx, W. Kleist, M. Hunger and A. Baiker, *J. Phys. Chem. Lett.*, 2010, **1**, 2886-2890.
42. K. Tan, N. Nijem, P. Canepa, Q. Gong, J. Li, T. Thonhauser and Y. J. Chabal, *Chem. Mater.*, 2012, **24**, 3153-3167.
43. L. Bellarosa, S. Calero and N. Lopez, *Phys. Chem. Chem. Phys.*, 2012, **14**, 7240-7245.
44. M. De Toni, R. Jonchiere, P. Pullumbi, F. X. Coudert and A. H. Fuchs, *ChemPhysChem*, 2012, **13**, 3497-3503.

